

**$^{197}\text{Au}(n,\gamma)$  Standard Cross Section and Experimental Data**

V.G. Pronyaev  
IPPE, Obninsk, Russia

$^{197}\text{Au}(n,\gamma)$  reaction cross section is used as standard for neutron cross section measurements in the energy range between 200 keV and 2.8 MeV. Last evaluation of this standard was completed in 2004 [1] and included in the IAEA and ENDF/B-VII standard files [2, 3]. ENDF/B-VII general purpose file is based on  $^{197}\text{Au}(n,\gamma)$  evaluation for standards including the energy range between 5 and 200 keV, where it was evaluated with account of the complete experimental data but not recommended as a standard. The evaluation of the  $^{197}\text{Au}(n,\gamma)$  standard cross section was done in the least-squares fit of all experimental data sets available for this cross section [1] including data sets for 21 absolute  $^{197}\text{Au}(n,\gamma)$  measurements, 6 shape  $^{197}\text{Au}(n,\gamma)$  cross section measurements, 3 measurements of absolute ratios to  $^6\text{Li}(n,\alpha)$  cross section, 3 measurements of absolute ratios to  $^{10}\text{B}(n,\alpha_1)$  cross section, 3 measurements of shape ratios to  $^{10}\text{B}(n,\alpha_1)$  cross section, 4 measurements of absolute ratios to  $^{10}\text{B}(n,\alpha)$  cross section, 9 measurements of absolute ratios to  $^{238}\text{U}(n,\gamma)$  cross section, 1 measurement of shape ratio to  $^{238}\text{U}(n,\gamma)$  cross section, 10 measurements of absolute ratios to  $^{235}\text{U}(n,f)$  cross section and 2 measurements of shape ratios to  $^{235}\text{U}(n,f)$  cross section. All standards database included more than 400 datasets for cross sections and their ratios reduced to the data of the types directly measured in the experiments.

The result of neutron standard evaluation is compared at the Figure 1 with the experimental data for absolute and shape measurements taken from the standards database and Ratynski and Käppeler evaluation [4] used as standard for normalization of capture cross sections measured for astrophysical applications. The ratio of last neutron standard evaluation to the Ratynski and Käppeler evaluation is shown at Figure 2. For astrophysical applications, the Maxwellian spectrum averaged cross sections in dependence from neutron temperature  $kT$  are most important. These data from the database for astrophysical applications KADoNIS [5], which are consistent with Ratynski and Käppeler [4] group cross sections and shown at Figure 2, are compared at Figure 3 with  $^{197}\text{Au}(n,\gamma)$  Maxwellian Averaged Cross Section (MACS) from ENDF/B-VII library file, where standard cross section is inserted for energies between 5 keV and 2.8 MeV.

Maxwellian spectrum averaged cross sections (MACS) can be calculated from the evaluated point-wise cross sections and compared with the results of direct measurements of this integral quantity. All calculations here were done with the code INTER (release 7.0) [6], which since release 6.12 uses “stellar” definition of MACS [4]:

$$\frac{\langle \sigma v \rangle}{v_T} = \frac{2}{\sqrt{\pi}} \frac{\int_0^{\infty} \sigma(E_n) E_n \exp(-E_n / kT) dE_n}{\int_0^{\infty} E_n \exp(-E_n / kT) dE_n},$$

where  $\sigma$  is the capture cross section,  $E_n$  and  $v$  are the neutron energy and velocity,  $T$  is the neutron temperature.

The direct measurements of MACS are based at some proximity of temperature Maxwellian spectrum with  $kT$  about 25 keV to neutron spectrum from  $^7\text{Li}(p,n)$  reaction for protons with an incident energy 1912 keV [4] and with  $kT$  about 5.1 keV to neutron spectrum from  $^{18}\text{O}(p,n)$  reaction for protons with an incident energy 1911 keV [7]. The only experimental data available are data at  $kT=25$  keV by Ratynski and Käppeler [4] taken from EXFOR entry X4=22099 and

multiplied at  $2/\pi^{1/2}$ , to convert Maxwellian averaged cross section in its “stellar” definition. Evaluation done by Ratynski and Käppeler [4] basing on these data is 4 – 8 % below the neutron standards evaluation in 10 – 100 keV region.

The reason of this discrepancy can be explained by the difference in the experimental data used in these evaluations. Ratynski and Käppeler [4] evaluation is based exclusively at R.L. Macklin’s experimental microscopic cross section data [8] corrected in 1982 and results of own measurements [4] of the MACS at  $kT=25$  keV. Contrary to this, the standards evaluation is based at 62 data sets for  $^{197}\text{Au}(n,\gamma)$  cross section and their ratios to other reaction cross sections, all used in the combined least-squares fit. Comparison of Macklin’s experimental data [8] measured relative  $^6\text{Li}(n,\alpha)$  cross section, but taken as they are given in the EXFOR library, with both evaluations is shown at Figure 4. As we see the standards evaluation is systematically higher than Macklin’s data. Figures 5 and 6 show the comparison of the evaluated standards and experimental data for ratios of the  $^{197}\text{Au}(n,\gamma)$  cross section. It is seen, that for ratio of  $^{238}\text{U}(n,\gamma)$  to  $^{197}\text{Au}(n,\gamma)$  cross sections measured below 100 keV is systematically higher than obtained in the least-squares fit of standards with inclusion of all data. The trend is in the same direction, requiring the possible decreasing of the  $^{197}\text{Au}(n,\gamma)$  cross section comparing with the standards least-squares fit, as it is observed with Macklin’s [8] result of ratio  $^{197}\text{Au}(n,\gamma)$  to  $^6\text{Li}(n,\alpha)$  cross section measurement. One of the possible reasons of these discrepancies is possibly the problems in the estimation of the sensitivity of the gamma detector in “old” ORELA measurements [9]. The problems appear when prompt gamma-ray spectra are varying substantially with neutron incident energy, as it is shown, for example, by O.A. Wasson et al. [10]. Large correction accounting the difference in the spectra of the registered gammas from  $^{197}\text{Au}(n,\gamma)$  and  $^{238}\text{U}(n,\gamma)$  reactions was introduced by Wisshak in the results of his ratio measurements presented in Fig. 6 as data sets DS430 and DS431. The uncertainty in determination of this correction is large and possibly can explain the inconsistency between results of measurements with total gamma-rays registration detectors and other detectors, sensitivity of which does not depend from gamma-ray spectra. There are detailed studies of these factors [11]. After careful analysis, the results obtained at n\_TOF facility with two types of detector ( $\text{C}_6\text{D}_6$  – total gamma-rays registration detector and TAC – total absorption calorimeter) for  $^{197}\text{Au}(n,\gamma)$  in the region of the resolved resonances have been appeared consistent in average within 2% [12] and also consistent with the preliminary results of the IRMM obtained independently with  $\text{C}_6\text{D}_6$  detector. Basing on this, we should expect, that the analysis in the region between 1 and 200 keV of the results of latest measurements in n\_TOF and IRMM will give the reliable data for this neutron energy.

The direct MACS measurements at  $kT=25$  keV for  $^{197}\text{Au}(n,\gamma)$  reaction were done with spectrum simulated in  $^7\text{Li}(p,n)$  reaction by protons having incident energy 1912 keV [4]. The authors [4] mention about good consistency between simulated and model Maxwellian spectrum with  $kT=25$  keV. This conclusion is based at good agreement of MACS calculated with Macklin’s [8] experimental cross section using model Maxwellian spectrum truncated for energies above 110 keV with MACS measured at simulated spectrum, which on kinematical limitations practically has no neutrons with energy above 110 keV. The temperature in  $kT=25.0\pm 0.5$  keV was assigned to the simulated spectrum because the model Maxwellian spectrum with the temperature 25.3 keV gives the best least-squares fit of measured simulated spectrum. Figure 7 shows the comparison of experimental data for simulated spectrum (see also Figure 3 in [4]) obtained from A. Mengoni [11] (data are in Table 1) with Maxwellian spectrum at two temperatures:  $kT=25.3$  keV and  $kT=28.5$  keV. The consistency of present data and calculations with data and calculations in [4] was checked by comparison of MACS value obtained for simulated spectrum above 3 keV folded with Macklin’s data and published in original paper [4] ( $568 \cdot (2/\pi^{1/2})$  mb) with the value obtained by us ( $561 \cdot (2/\pi^{1/2})$  mb) using same spectrum [11] and Ratynski and Käppeler recommended  $^{197}\text{Au}(n,\gamma)$  cross section [4]. Because Ratynski and Käppeler  $^{197}\text{Au}(n,\gamma)$

cross section evaluation are the energy-group presentation of Macklin's data [11] multiplied at 0.989 normalization coefficient, the consistency between two is good.

The statement that Maxwellian spectrum with  $kT=25$  keV reproduces by the best way the experimental simulated spectrum has a few shortcomings. First of all, the closeness between two MACS integral values does not obligatory mean the closeness of the neutron spectra under the integral. The least-squares fit done by authors with minimization as we may guess of sum of squares of differences between the model and simulated spectrum with practically equal bins on neutron energy leads to some reduction of the effective temperature for simulated spectra. If we calculate the average energy of simulated spectrum, it will be equal to 42.75 keV (or  $kT=28.5$  keV). As we see from Figure 7, Maxwellian spectrum with  $kT=28.5$  keV fits better the spectrum in the energy range below 80 keV. The maximum of the simulated spectrum is located near 30 keV, but not at 25 keV as for true Maxwellian spectrum with  $kT=25$  keV. From our point of view, a more consistent way for presentation of MACS experimental data obtained with given simulation spectrum is: i) to fit the simulated spectrum with true Maxwellian one in more narrow energy range near the maximum of the spectra (e.g. 0 – 80 keV) than it was done in [4] (0 – 110 keV), ii) to assign to the simulated spectrum the temperature value of the adjusted Maxwellian spectrum and iii) to correct obtained MACS at the differences between true Maxwellian and simulated spectrum. Although the correction factor can be in this case larger than in [4], the effective temperature and MACS obtained with simulated spectrum will present more realistically the temperature and MACS value for true Maxwellian spectrum.

To show this, the following calculations have been done for simulated spectra shown on Figure 7. The spectrum averaged values for  $^{197}\text{Au}(n,\gamma)$  cross section from ENDF/B-VII library were calculated for experimental simulated spectrum (713.9 mb) and for true Maxwellian spectra at  $kT=25$  (682.4 mb) and 28.5 keV (633 mb). Then the experimental value of MACS (586 mb) converted in the astrophysical definition and corrected at the differences in the spectra can be obtained for temperature assigned to  $kT=25$  keV as:  $586 \cdot (2/\pi^{1/2}) \cdot 682.4/713.9 = 632.1$  mb and for temperature assigned to  $kT=28.5$  keV as:  $586 \cdot (2/\pi^{1/2}) \cdot 633/713.9 = 586.3$  mb. If we will use Ratynski and Käppeler [4] evaluation for introducing of the correction at the differences in the spectra, we will obtain accordingly 632.2 mb and 585.3 mb. This shows, that the calculated correction at the difference between simulated and true Maxwellian spectra is insensitive to small variations in the cross sections used for calculations of the correction.

Results obtained in present analysis of  $^{197}\text{Au}(n,\gamma)$  MACS measured with simulated spectrum (586.3 mb at  $kT=28.5$  keV and 632 mb at  $kT=25$  keV) can be compared with the results recommended in [4] (601.8 mb for  $kT=28.5$  keV if interpolate between 25 and 30 keV, and  $648 \pm 10$  mb for  $kT=25$  keV). As it is seen, MACS experimental value for  $kT=25$  keV estimated here is about 2.5% below value obtained in [4]. This difference is partly due to different correction procedures used: here in calculations of correction we used simulated spectrum in the energy range where it was non-zero (0.5 keV – 118 keV) and in [4] for the energy range above 3 keV was used. Because the region below 3 keV contributes about 3% in the  $^{197}\text{Au}(n,\gamma)$  MACS for  $kT=25$  keV and deviations of simulated from true Maxwellian spectrum are large (see Figure 7) it should be accounted in the calculation of the correction. MACS measured values derived here are at 8% below ENDF/B-VII calculated values: 633 mb at  $kT=28.5$  keV and 682.4 at  $kT=25$  keV.

The energy group averaged cross sections and MACS for  $^{197}\text{Au}(n,\gamma)$  evaluated for standards in comparison with Ratynski and Käppeler [4] recommendation are given in Tables 2 and 3. Values in brackets given in Table 2 show the MACS calculated from the  $^{197}\text{Au}(n,\gamma)$  file of ENDF/B-VII library where values from standards evaluation between 5 keV and 2.8 MeV were used in the file. More low MACS values for low  $kT$  obtained for ENDF/B-VII file in comparison with cross

section recommended for Russian Reactor Dosimetry File (RRDF-2007) is explained by some loss of capture areas observed mainly near upper boundary (5 keV) of the resolved resonance region used in the file of the ENDF/B-VII library. To account this loss, the statistical model calculations were done with EVPAR code and average parameters for s- orbital wave given in the resolved resonance region and p- and d- waves average parameters adjusted to fit the total capture cross section. The results of these calculations are shown in Figure 8. We see that the average contribution from p-, d-wave resonances in the capture cross section is more than 1% for energy above 1 keV reaching 8% at 5 keV. This contribution from many resonances with low neutron widths is not accounted in the ENDF/B-VII evaluation. The statistical analysis of resonances in the resolved resonance region shows also some loss of s- resonances near upper boundary of the resolved resonance region. As result, the  $^{197}\text{Au}(n,\gamma)$  evaluation from ENDF/B-VII library shown in the group presentation gives too low cross sections above 3 keV. To correct this, the upper boundary of the resolved resonance region for RRDF-2007 was reduced to 4.8 keV, the smooth background cross section shown at Figure 8 as contribution from p-, d- and f-waves was added in the resolved resonance region and 8 fictitious s- resonances with neutron width 0.2 eV and gamma width 0.124 eV were added in the energy range from 4 to 4.8 keV to compensate the loss (about 20%) of s-resonances in this energy region. Standard evaluation (as in ENDF/B-VII library) was used in the energy range from 5 keV to 2.8 MeV and ENDF/B-VII evaluation for energy above 2.8 MeV. Values of the group averaged cross sections for RRDF-2007 and MACS evaluated for RRDF-2007 in comparison with KADoNIS [7] recommendation are given in Tables 2 and 3. Typically they are about 5 – 7% higher in the kT range 15 – 25 keV.

The file of uncertainties for  $^{197}\text{Au}(n,\gamma)$  reaction in the RRDF-2007 library consists from 3 components: covariance matrix of uncertainties obtained in the standards combined evaluation in the energy range between 4.8 keV and 2.6 MeV, covariance matrix of uncertainties calculated from uncertainties of the resolved resonance parameters with account of missed resonances for the energy range  $10^{-5}$  eV to 4.8 keV and covariance matrix of the uncertainties estimated from the uncertainties of the experimental data for the energy range from 2.6 MeV to 20 MeV.

The revisioin of the evaluated  $^{197}\text{Au}(n,\gamma)$  cross section in keV region does not influence much at the reaction rates of systems with thermal neutron spectrum, but increases substantially the reaction rates for capture reaction cross sections in keV region measured relative  $^{197}\text{Au}(n,\gamma)$  and used in astrophysical applications.

The results for other reactions contributing in the improvement of  $^{197}\text{Au}(n,\gamma)$  cross section through ratio measurements in the energy range 1 to 200 keV are shown in Fig. 9 to 13 for completeness.

## References

1. International Evaluation of Neutron Cross-Section Standards, IAEA Special Technical Report, STI/PUB/1291, IAEA, Vienna (2007).
2. <http://www-nds.iaea.org/standards/data.html> (2007).
3. <http://www.nndc.bnl.gov/exfor7/4web/zips/std-ENDF-VII0.endf.zip> (2007).
4. W. Ratynski, F. Käppeler, Phys. Rev., C37, 595 (1988).
5. Karlsruhe Astrophysical Database of Nucleosynthesis in Stars, <http://nuclear-astrophysics.fzk.de/kadonis/> (2007).
6. <http://www-nds.iaea.org/ndspub/ndf/utility/index.htmlx> (2007).
7. M. Heil, N. Winckler, S. Dababneh et al., Nucl. Phys., A758, 529c (2005).
8. R.L. Macklin, Nucl. Sci. and Eng., 79, 265 (1981).
9. K.H. Guber, L.C. Leal, R.O. Sayer et al., in Proc. of Intern. Conf. on Nucl. Data for Sci. and Technology, Santa Fe, N.M., 26 September – 1 October 2004, AIP Conf. Proceedings No. 769, 1706 (2005).

10. O.A. Wasson, R.E. Chrien, M.R. Bhat et al., Phys. Rev., 173, 1170 (1968).
11. A. Borella, J. Aerts, F. Gunsing et al., Nucl. Instr. and Meth. in Phys. Res., A577, p. 626 (2007).
12. M. Massimi et al. (n\_TOF collaboration), in Proc. of the Int. Conf. on Nucl. Data for Sci. and Technology, Apr. 22 – 27, 2007, Nice, France, p. 1265 (2008).
13. A. Mengoni, Private Communication (October 2007).

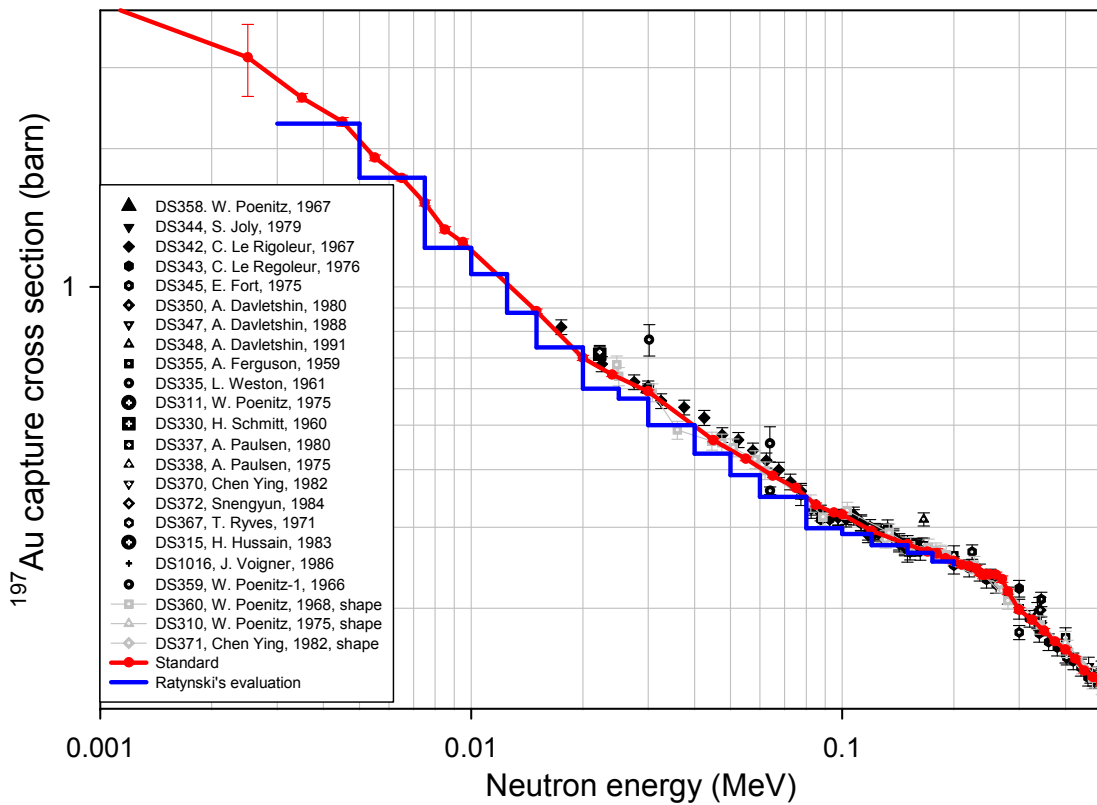


Fig. 1. Comparison of the  $^{197}\text{Au}(n,\gamma)$  standard evaluation with Ratynski and Käppeler [4] evaluation and experimental data for absolute cross section measurements.

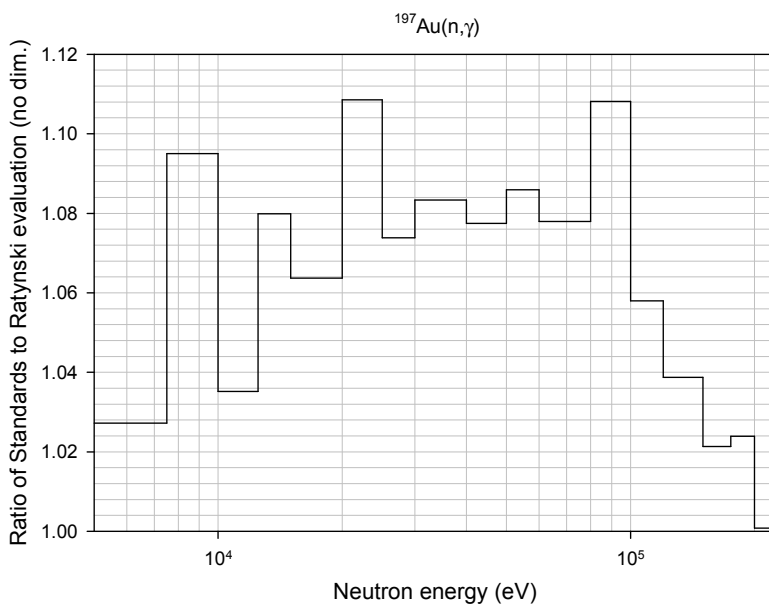


Fig. 2. Ratio of the standards evaluation to the Ratynski and Käppeler [4] evaluation.

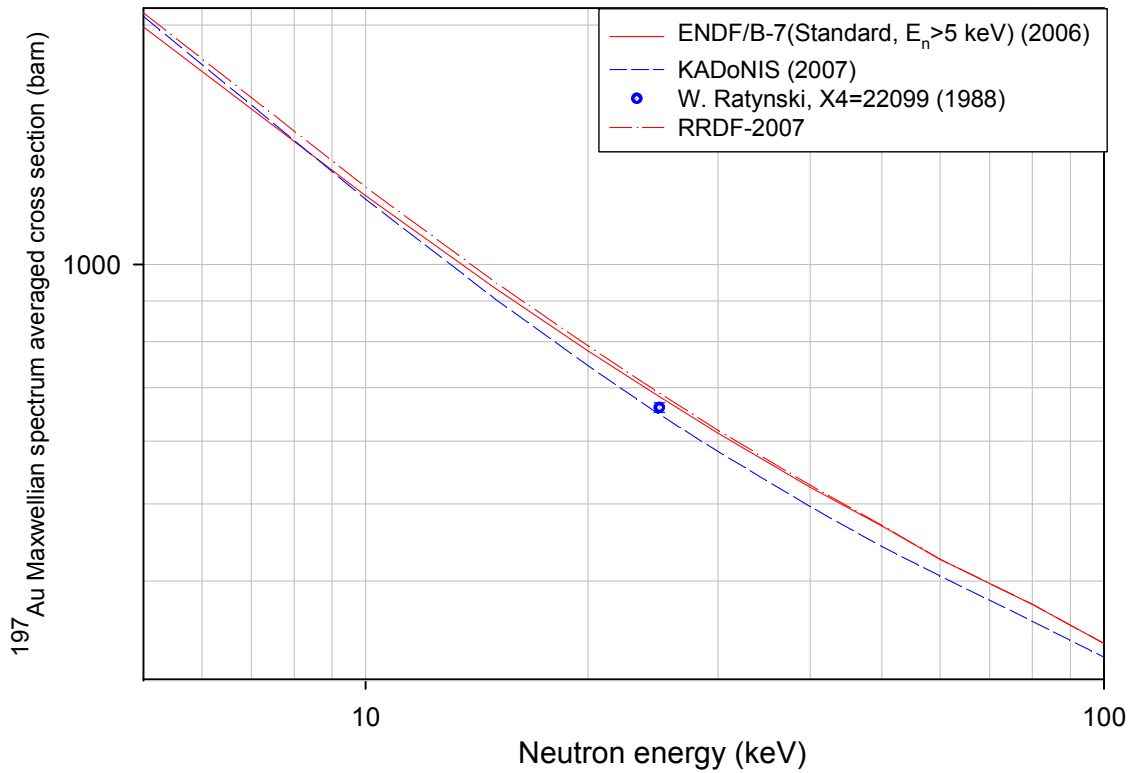


Fig. 3. Comparison of MACS for  $^{197}\text{Au}(n,\gamma)$  ENDF/B-VII and RRDF-2007 (explanations are evaluation with Ratynski and Käppeler [4] evaluation and their experimental data for simulated spectra with  $kT$  assigned to 25 keV).

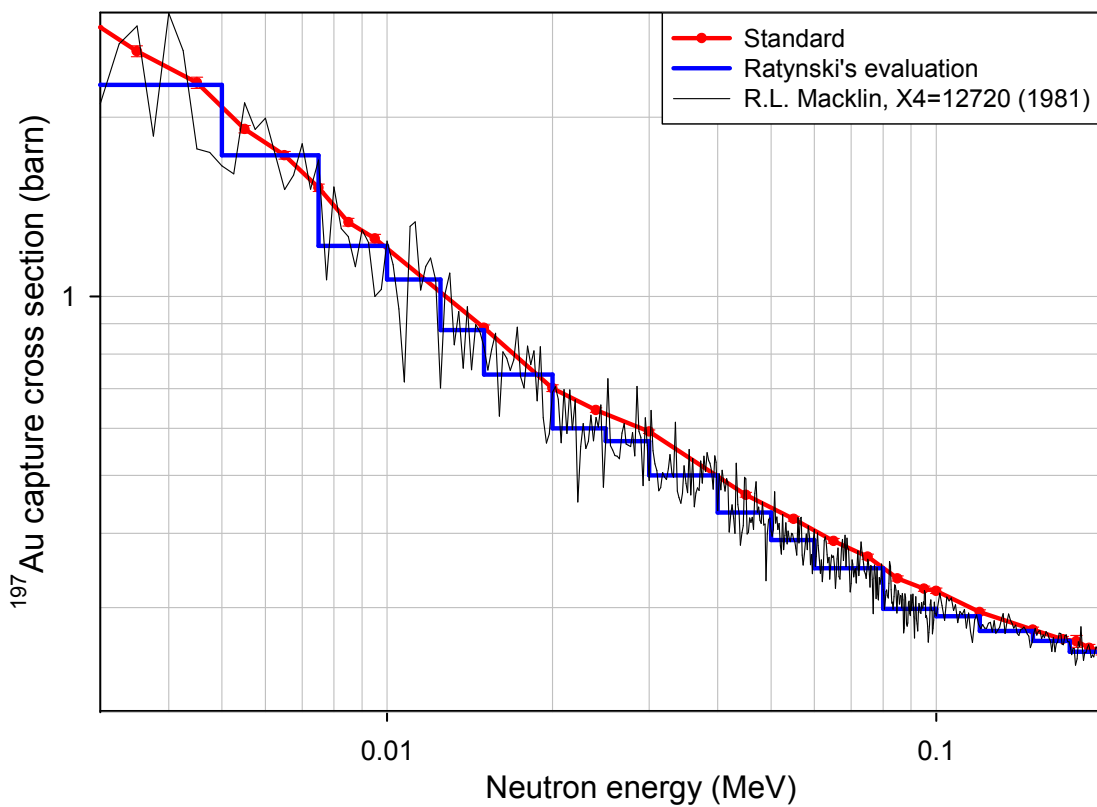


Fig. 4. Comparison of the  $^{197}\text{Au}(n,\gamma)$  standard evaluation with Ratynski and Käppeler [4] evaluation and Macklin's experimental data taken from EXFOR library.

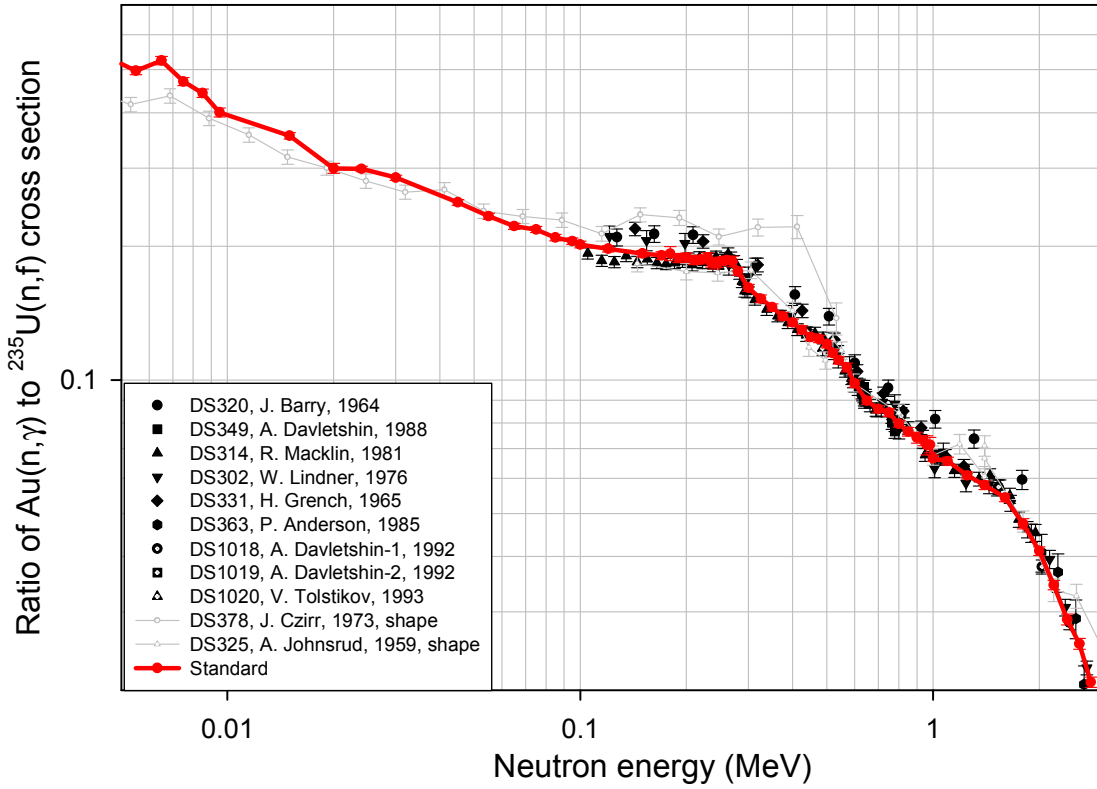


Fig. 5. Comparison of the  $^{197}\text{Au}(n,\gamma)/^{235}\text{U}(n,f)$  ratio of standard evaluation with experimental data.

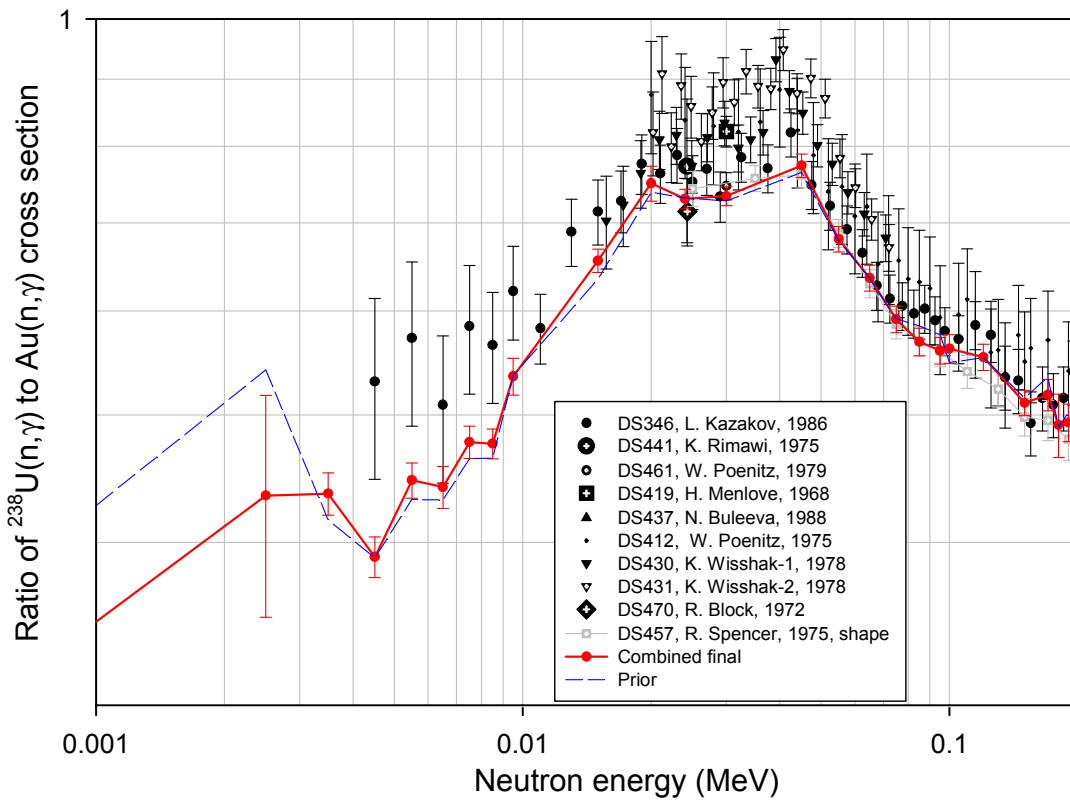


Fig. 6. Comparison of the  $^{238}\text{U}(n,\gamma)/^{197}\text{Au}(n,\gamma)$  ratio of standard evaluation with experimental data.

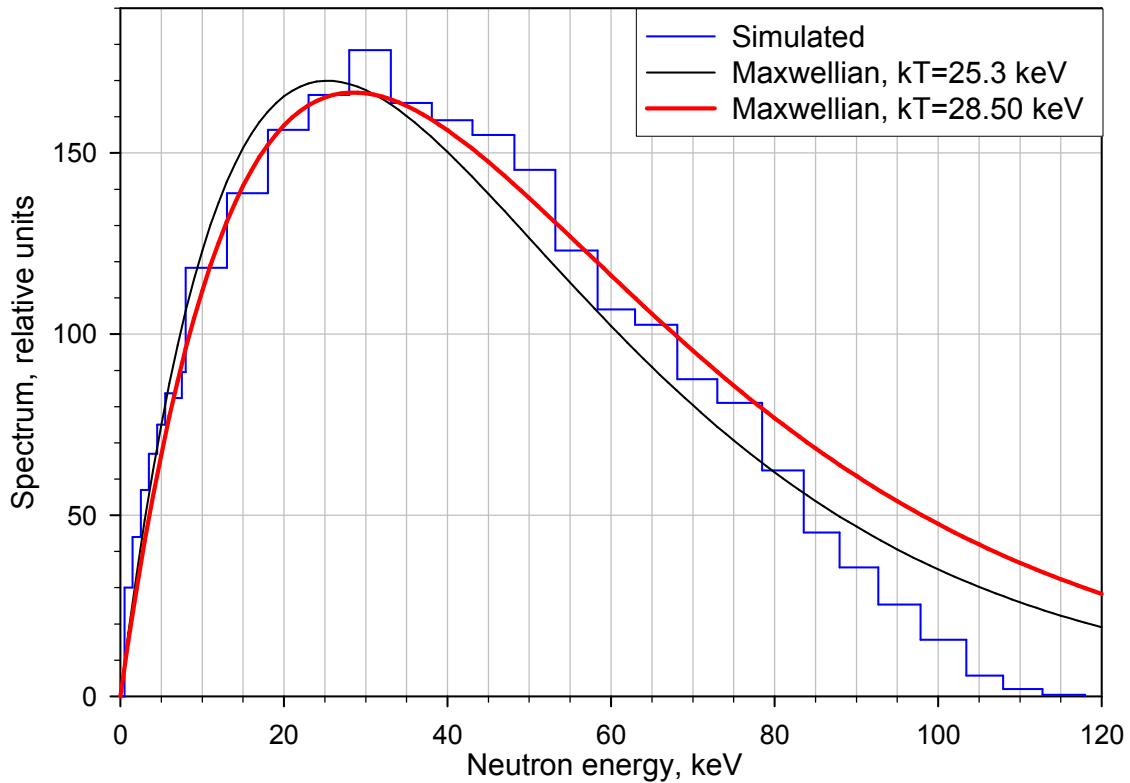


Fig 7. Comparison of experimental simulated neutron spectrum with “true” Maxwellian neutron spectrum for two temperatures  $kT=25.3$  and  $28.5$  keV. All spectra have free normalization.

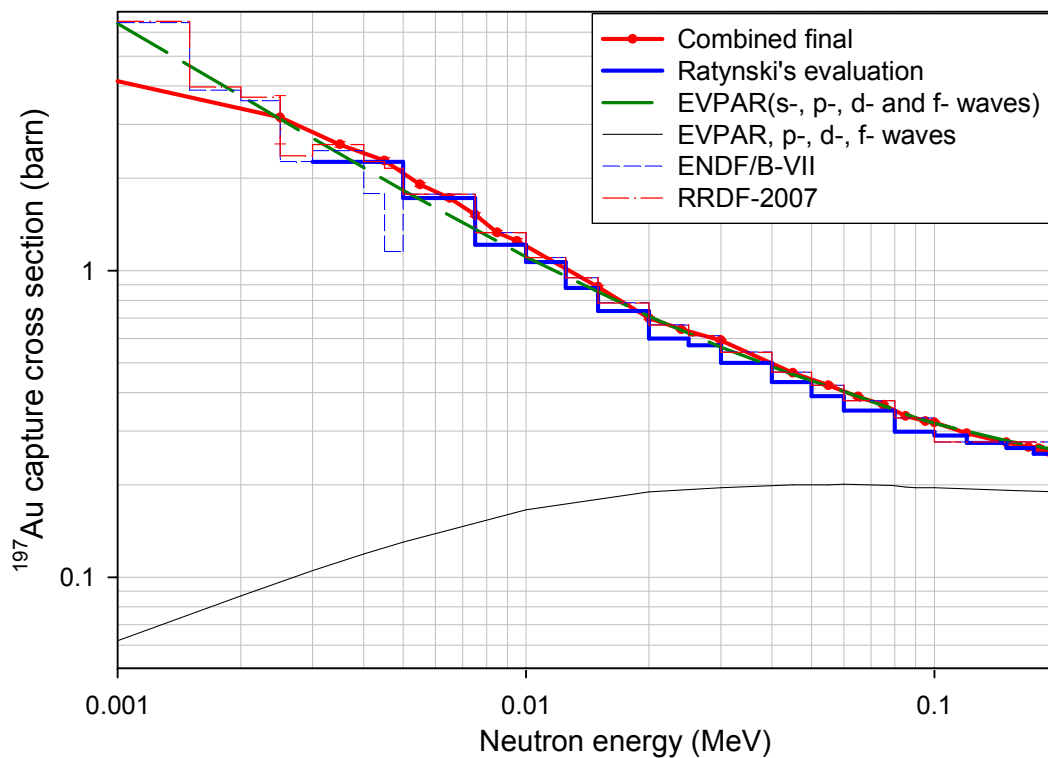


Fig. 8. Comparison of the results of the statistical model calculations (long-dash and thin solid smooth curves - contribution of different orbital waves) with Ratynski and Käppeler evaluation [4] (thick line histogram), standards evaluation [1] (thick line), ENDF/B-VII evaluation (short-dash line histogram) and RRDF-2007 (dash-dot histogram).

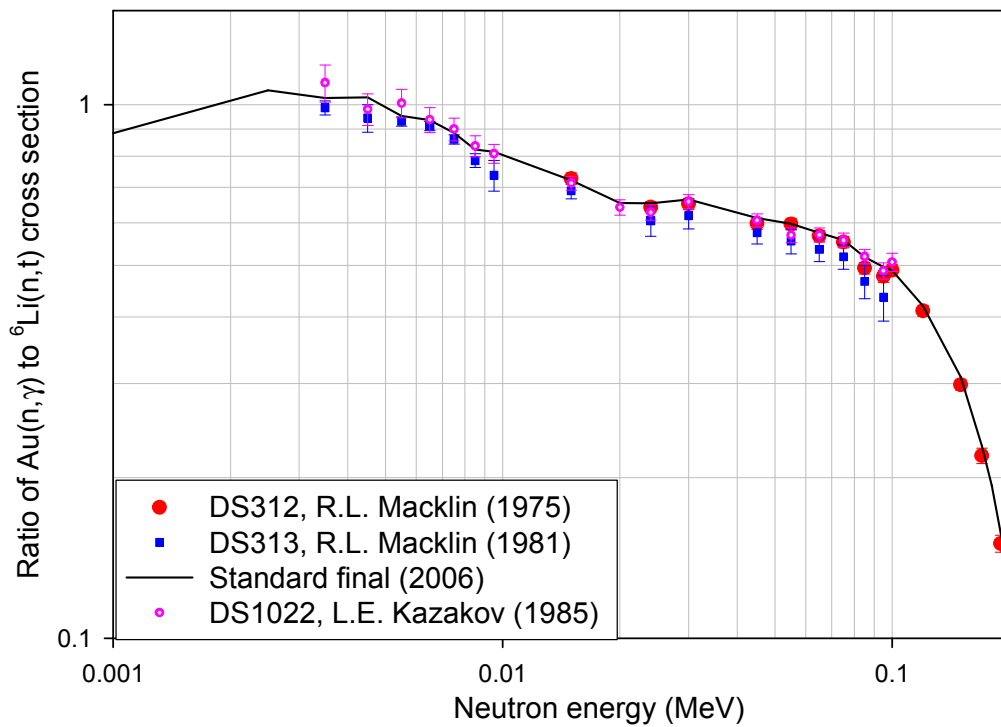


Fig 9. Comparison of the ratio of  $^{197}\text{Au}(n,\gamma)/^6\text{Li}(n,t)$  standard evaluation in the energy range 1 keV – 200 keV with experimental data by R.L. Macklin.

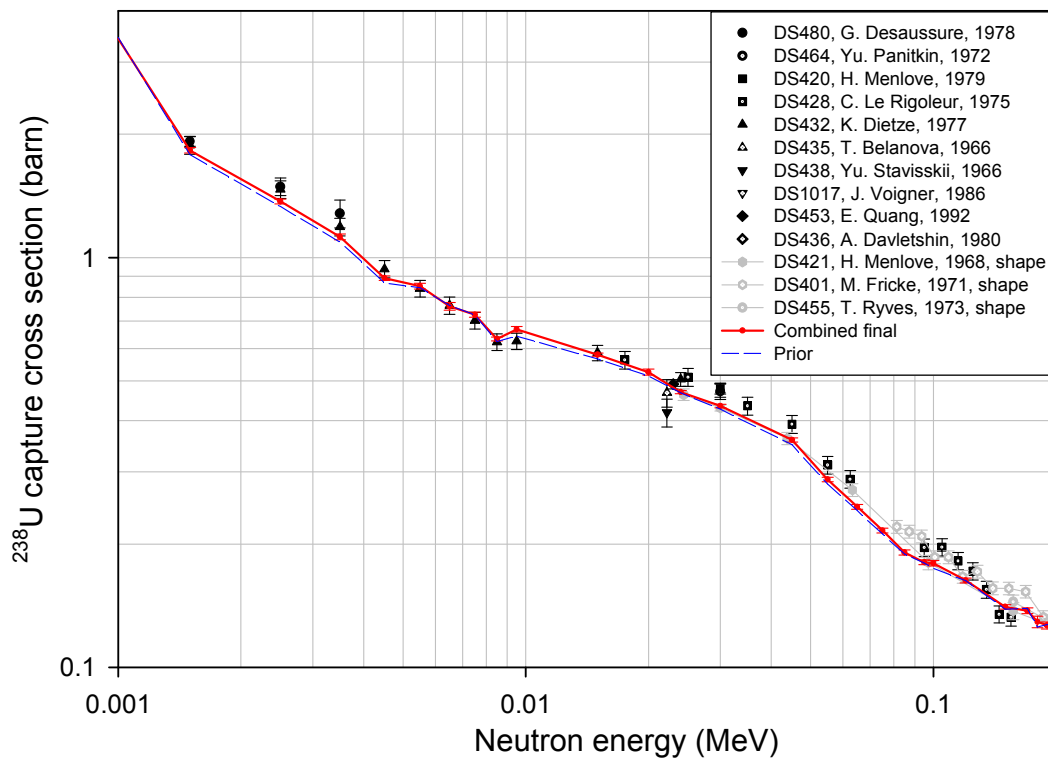


Fig 10. Comparison of  $^{238}\text{U}(n,\gamma)$  standard evaluation in the energy range 1 keV – 200 keV with experimental data.

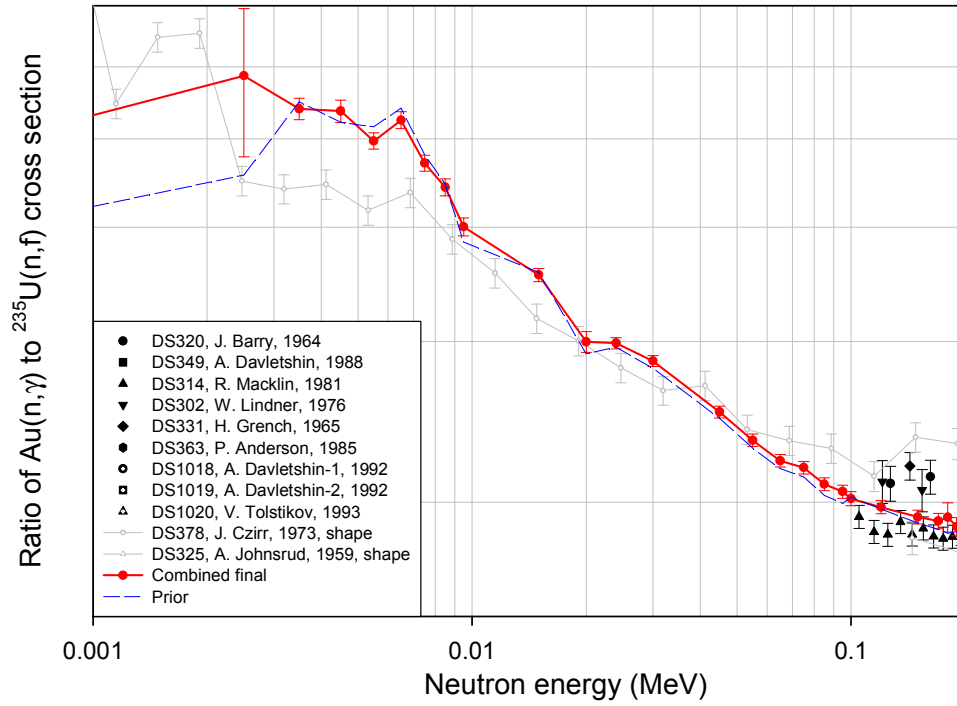


Fig 11. Comparison of the ratio of  $^{197}\text{Au}(n,\gamma)/^{235}\text{U}(n,f)$  standard evaluation in the energy range 1 keV – 200 keV with experimental data.

Table 1. Experimental neutron spectrum from  ${}^7\text{Li}(p,n)$  reaction at 1912 keV proton energy [11] (see also Fig.3 in [4]).

Neutron energy: left boundary of the group, keV	Neutron energy: right boundary of the group, keV	Spectrum, relative units
0.00000001	0.5	0.0
0.5	1.5	30.
1.5	2.5	44.
2.5	3.5	57.
3.5	4.5	67.
4.5	5.5	75.
5.5	6.5	83.7
6.5	7.5	82.3
7.5	8.01	89.5
8.01	13.023	118.3
13.023	18.026	138.9
18.026	23.002	16.4
23.002	27.964	166.
27.964	33.083	178.4
33.083	38.067	163.8
38.067	43.068	159.0
43.068	48.183	155.0
48.183	53.175	145.3
53.175	58.363	123.1
58.363	62.941	106.8
62.941	68.080	102.6
68.080	73.002	87.6
73.002	78.479	81.0
78.479	83.572	62.4
83.572	87.926	45.2
87.926	92.680	35.6
92.680	97.832	25.3
97.832	103.43	15.6
103.43	107.94	5.72
107.94	112.76	1.98
112.76	117.98	0.4
117.98	20000.0	0.0

Table 2. Group averaged  ${}^{197}\text{Au}(n,\gamma)$  cross section from the standards evaluation in comparison with Ratynski and Käppeler evaluation [4].

En, keV	$\langle\sigma\rangle$ , mb [4]	$\langle\sigma\rangle$ , mb standards
5-7.5	1726.7	1773.7
7.5-10	1215.7	1331.2
10-12.5	1066.7	1104.2
12.5-15	878.0	948.1
15-20	738.8	785.0
20-25	600.0	665.2

25-30	570.8	613.0
30-40	500.4	542.1
40-50	433.3	466.9
50-60	389.6	423.1
60-80	349.4	376.6
80-100	298.3	330.6
100-120	290.1	306.9
120-150	274.1	284.7
150-175	263.7	269.3
175-200	252.6	258.7
200-225	248.5	248.7

Table 3.  $^{197}\text{Au}(n,\gamma)$  MACS from RRDF-2007 and ENDFB-VII (values given in the brackets of last column) libraries in comparison with Ratynski and Käppeler evaluation [4] and calculated from ENDF/B-VII file with cross sections replaced at group cross sections by Ratynski and Käppeler [4] given in Table 2.

kT, keV	$\langle\sigma\rangle$ [4], mb	$\langle\sigma\rangle$ [4] in ENDF/B-VII shell, mb	$\langle\sigma\rangle$ RRDF-2007 mb
5	2050	1983	2066 (1990)
10	1208	1184	1250 (1221)
15	904	892	949 (933)
20	746	738	790 (779)
25	648	643	689 (682)
30	582	577	619 (614)
40	496	493	528 (525)
50	442	442	470 (469)
60	406	403	426 (426)
80	356	357	374 (374)
100	321	320	334 (334)